

## GREENWOODITE, A NEW NESOSILICATE FROM BRITISH COLUMBIA WITH A Ba-VOH COUPLED SUBSTITUTION AND TETRAHEDRAL Fe: DESCRIPTION AND STRUCTURE

PAUL R. BARTHOLOMEW<sup>§</sup>

*Department of Biology and Environmental Science, University of New Haven, 300 Boston Post Rd, West Haven, CT 06516*

FRANCO MANCINI

*U.O. Geologia, Italferr s.p.a., Via Marsala 53, 00185 - Rome, Italy*

GEORGE E. HARLOW

*Earth and Planetary Sciences, American Museum of Natural History, Central Park West at 79th Street, New York, NY  
 10024-5192*

NICHOLAS DEIFEL AND CHRISTOPHER CAHILL

*Department of Chemistry, George Washington University, 725 21st Street NW, Washington, DC 20052*

HEINZ-JUERGEN BERNHARDT

*Zentrale Elektronen-Mikrosonde, Ruhr-University Bochum, Universitätsstraße 150, 44801 Bochum, Germany*

### ABSTRACT

Greenwoodite, ideal formula  $\text{Ba}_{2-x}(\text{V}^{3+}\text{OH})_x\text{V}_9(\text{Fe}^{3+}, \text{Fe}^{2+})_2\text{Si}_2\text{O}_{22}$ , space group  $P\bar{3}m1$ ,  $a$  5.750(1) Å,  $c$  14.459(1) Å,  $V$  414.00(8) Å<sup>3</sup>,  $Z = 1$ , is a new mineral from the Wigwam deposit of Southeastern British Columbia, Canada. It is a metamorphic mineral formed under greenschist-facies conditions as part of an assemblage that includes quartz, celsian, apatite, sphalerite, pyrrhotite, galena, pyrite, zoltaitite, and batisivite. Greenwoodite has a Mohs hardness of 5, one perfect cleavage, a semi-prismatic to tabular habit, and a calculated density of 4.81 g/cm<sup>3</sup>. It is opaque with reflectance and color similar to those of sphalerite. The strongest eight lines of the calculated X-ray powder diffraction pattern [ $d$  in Å ( $h k l$ )] are 2.925(100)(0 1 4), 2.875(38)(1 1 0), 2.672(23)(1 1 2), 2.469(35)(1 1 3), 2.354(28)(2 0 2), 2.212(28)(2 0 3), 1.669(26)(1 2 4), and 1.438(35)(2 2 0). The empirical formula, derived from microprobe analysis and the crystal structure, is  $\text{Ba}_{0.60}(\text{V}^{3+}\text{OH})_{0.40}(\text{V}^{3+}_{8.33}, \text{Cr}_{0.33}, \text{Ti}_{0.13}, \text{Al}_{0.13}, \text{Mn}^{3+}_{0.02})_{\Sigma 9}(\text{Fe}^{3+}_{1.08}, \text{Fe}^{2+}_{0.60}, \text{Zn}_{0.22}, \text{Al}_{0.06}, \text{Mg}_{0.04})_{\Sigma 2}(\text{Si}_{1.72}, \text{Fe}^{3+}_{0.28})_{\Sigma 2}\text{O}_{22}$ . The crystal structure was solved using direct methods for the location of Ba, V, and Fe and using Patterson synthesis and Fourier maps for the positions of the Si and O. The final  $R$  factor was 1.9% using 475 unique observed reflections. The structure is based on hexagonal closest packing (hcp) of oxygen atoms with 4 distinct cation layers designated BV, V1, V2, and V3 having a stacking sequence BV-V1-V2-V3-V2-V1-BV-V1-... The core layers (all layers except BV) contain 3 distinct V-dominated sites, one tetrahedral Si site and one Fe-dominated tetrahedral site containing a disordered mixture of equal amounts of trivalent and divalent cations. The BV layer is a disordered mixture of 2 endmember layer structures related by the coupled substitution  $2\text{Ba}^{2+} = 2\text{O}^{2-} + 2\text{V}^{3+} + 1\Box + 2\text{H}^+$ . In the Ba endmember the Ba is at a cubo-octahedral site formed by a hole in one of the hcp oxygen layers. In the VOH endmember the Ba is replaced by an O atom which forms the shared corner of a triplet of octahedral sites. Only 2/3 of these sites are occupied, predominantly by V. Charge balance is achieved by bonding H to this O atom. The composition of the type grain of greenwoodite is 60% toward the Ba endmember of this coupled-substitution solid solution.

<sup>§</sup> E-mail address: pbartholomew@newhaven.edu

## INTRODUCTION

Greenwoodite is the second new mineral discovered from the Wigwam deposit of southeastern British Columbia. It is compositionally and structurally distinct, but compositionally related to zoltaiite, the first new mineral described from this locality (Bartholomew *et al.* 2005). The new species and the name have been approved by the IMA Commission on New Minerals, Nomenclature, and Classification (IMA No. 2010-007, Bartholomew *et al.* 2010). The type specimen has been deposited with the American Museum of Natural History under catalogue number 109839. The name is in honor of Hugh J. Greenwood, retired professor and former head of the Geological Sciences Department at the University of British Columbia, Vancouver, BC, Canada. Dr. Greenwood is widely known for his pioneering work on developing the theory and experimental methods used to elucidate the role of mixed H<sub>2</sub>O-CO<sub>2</sub> fluids in metamorphic processes as well as pioneering work on developing algebraic methods and quantitative modeling methods used to understand and characterize petrologic processes and relationships. A summary of his work and essential publications can be found in Gordon (1991).

## OCCURRENCE AND PARAGENESIS

The Wigwam deposit is a metamorphosed Mississippi-Valley type base-metal deposit located in the Akolkolex River area southeast of Revelstoke, British Columbia (Thompson 1972, 1978). The deposit occurs in a silicified zone of the Cambrian-age Badshot Formation. Grain size, polyhedral grain boundaries (Fig. 1), and the general lack of secondary mineralization indi-

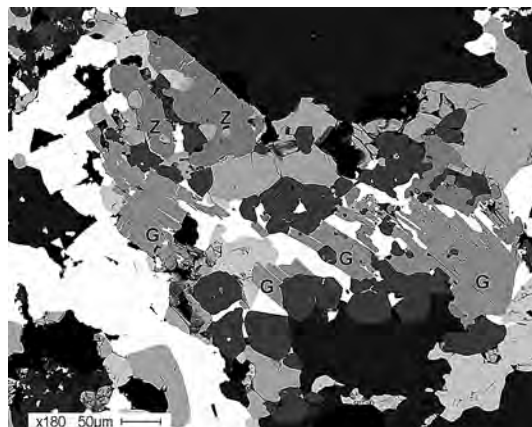


FIG. 1. Backscattered-electron (BSE) micrograph of greenwoodite grains (G) in matrix, showing semi-prismatic form and prominent cleavage. Grains of zoltaiite (Z) are also present in the field of view.

cate that greenwoodite is part of a prograde metamorphic assemblage whose P-T conditions of formation have been estimated to be 2 to 5 kbars and 300 to 425 °C (Bartholomew *et al.* 2005).

Greenwoodite occurs as part of a suite of three V-Ba-Si oxide minerals, the other two being zoltaiite and batisivite. All three of these minerals occur as trace phases within an assemblage of quartz, celsian, apatite, sphalerite, pyrrhotite, galena, and pyrite. Greenwoodite occurs as small, disseminated semi-prismatic to tabular grains. Irregular grains intergrown with other phases are common as well. One direction of cleavage is generally visible parallel to the longest dimension of the grains (Fig. 1). Grain sizes range from 40 to 200 µm for the longest dimension and 20 to 100 µm in width. Grains are occasionally isolated, but often occur in groups of 2 to 10 closely spaced grains of Ba-V-Si minerals (zoltaiite, batisivite, greenwoodite).

## PHYSICAL AND OPTICAL PROPERTIES

Greenwoodite is black and opaque with a submetallic to dull luster. It has one perfect cleavage with {001} orientation. Its Mohs hardness is estimated to be 5 based upon edge-relief formation and scratch resistance in polished sections compared to adjacent known minerals. The measured chemical composition and unit-cell dimensions (see below) yield a calculated density of 4.81 g/cm<sup>3</sup>. In reflected light greenwoodite has a low reflectance (similar to that of sphalerite), a gray color with a weak brownish tint, no internal reflections, and distinct bireflectance, pleochroism, and anisotropy with straight extinction relative to its cleavage direction. Reflectance measurements were made with a custom-made reflectance microscope that uses 16 single-line interference filters (half-width 10 nm) with peak wavelengths between 400 nm and 700 nm in steps of 20 nm. The objective in air and immersion oil is 20× with an effective numerical aperture of 0.18 in air and in oil. The reflectance standard was SiC #878. Leitz immersion oil conforming to DIN 58884 was used. Color is given for illuminant C. The results are in Table 1.

## CHEMICAL COMPOSITION

*Microprobe Analyses*

Electron microprobe analyses were performed using the Cameca SX-100 at the American Museum of Natural History. Beam conditions were 20 kV and 20 nA with a 2 µm beam diameter. Care was taken to avoid spectral interferences between BaMα-TiKα, TiKβ-VKα, and VKβ-CrKα. The standards used were as follows: synthetic MgCr<sub>2</sub>O<sub>4</sub> (Mg, Cr), synthetic MgAl<sub>2</sub>O<sub>4</sub> (Al), fayalite (Si), ilmenite (Ti, Fe), benitoite (Ba), synthetic V<sub>2</sub>O<sub>3</sub> (V), rhodonite (Mn), and synthetic ZnS (Zn). The results are presented in Table 2. The

TABLE 1. GREENWOODITE REFLECTANCE (%) AND COLOR VALUES IN AIR AND IMMERSION OIL

Wavelength (nm)	air $R_1$	air $R_2$	oil $R_1$	oil $R_2$
400	13.40	16.70	5.19	6.05
420	12.86	16.19	3.01	5.32
440	12.67	16.00	2.91	5.01
460	12.54	15.81	2.82	4.86
470*	12.50	15.75	2.82	4.83
480	12.49	15.73	2.82	4.81
500	12.46	15.62	2.83	4.78
520	12.44	15.53	2.85	4.74
540	12.53	15.57	2.97	4.80
546*	12.53	15.50	2.98	4.80
560	12.60	15.55	3.00	4.82
580	12.80	15.67	3.12	4.91
589*	12.81	15.75	3.31	4.95
600	13.04	15.81	3.25	5.00
620	13.26	15.97	3.41	5.12
640	13.52	16.15	3.52	5.23
650*	13.60	16.22	3.57	5.28
660	13.71	16.31	3.62	5.34
680	13.92	16.56	3.75	5.53
700	14.36	17.09	6.31	6.04
Color Values				
x	0.3173	0.3154	0.3242	0.3221
y	0.3246	0.3223	0.3324	0.3294
Y(%)	18.16	16.94	6.14	5.21
Ld	575	575	575	576
Pe	4.19	3.08	8.12	6.77

\* Interpolated value

quantities in Table 2 which were not measured directly are as follows: oxygen was calculated by stoichiometry, cation APF (atoms per formula) values were calculated by normalizing the sum of all cations (except hydrogen) to 15.0, and the presence of hydrogen in the structure was suspected based upon slightly low microprobe totals and the charge balance requirements of the structural formula and has been confirmed by FTIR (see below). The amount of hydrogen, as  $H_2O$ , is calculated, for the compositional averages only, based upon the structural formula. Although the microprobe analysis software only allows for one valence state of each cation, the structural formula and charge balance both imply that Fe is present in both  $Fe^{2+}$  and  $Fe^{3+}$  states and allows for calculation of the proportions of each that are present. These calculated amounts, as FeO and  $Fe_2O_3$ , are presented along with an updated analytical total which takes into account the change in the amount of O implied by stoichiometry.

#### Fourier-Transform Infrared Spectroscopy (FTIR)

FTIR spectra were gathered using a Thermo Nicolet Continuum IR Microscope coupled to a Thermo

Nicolet Nexus 670 IR Spectrometer at the American Museum of Natural History in order to verify the presence of hydrogen in the structure. Spectra were gathered in diffuse reflectance mode on greenwoodite in polished section using aluminum as a background standard. A dry nitrogen flush was used to minimize the contribution of atmospheric  $H_2O$ . Figure 2 shows an FTIR spectra of greenwoodite in the region between 3000 and 4000  $cm^{-1}$ , which is the only region where an absorption peak that could be attributed to a hydrogen bond was found. The peak at about 3495  $cm^{-1}$  is consistent with an O–H stretching vibration of H present as OH (*e.g.*, Rossman 1988).

#### STRUCTURE DETERMINATION

Grains of greenwoodite were needle-extracted by hand from polished sections and mounted on glass fibers using Ambroid cement. Mounted grains were screened for sharpness of diffraction spots using a Rigaku DMAX-Rapid Microdiffraction unit at the American Museum of Natural History. Single-crystal XRD data was obtained at George Washington University using a Bruker SMART diffractometer equipped with an

TABLE 2. ELECTRON MICROPROBE COMPOSITIONS

	Average of 21 analyses: 13 grains			Average of 3 analyses: Type grain		
	Oxides	StdDev	APF	Oxides	StdDev	APF
MgO	0.11	0.03	0.033	0.12	0.004	0.037
Al <sub>2</sub> O <sub>3</sub>	0.91	0.08	0.212	0.78	0.063	0.185
SiO <sub>2</sub>	8.63	0.09	1.717	8.60	0.015	1.724
TiO <sub>2</sub>	1.05	0.14	0.158	0.89	0.007	0.134
V <sub>2</sub> O <sub>3</sub>	58.03	0.75	9.255	57.13	0.004	9.182
Cr <sub>2</sub> O <sub>3</sub>	1.42	0.55	0.223	2.07	0.102	0.328
MnO	0.11	0.01	0.018	0.11	0.006	0.019
FeO	11.92	0.25	1.982	11.69	0.052	1.960
ZnO	1.52	0.12	0.223	1.52	0.009	0.225
BaO	15.13	0.64	1.180	15.36	0.059	1.206
Raw Total	98.83	0.32		98.28	0.083	
H <sub>2</sub> O	0.62		0.820	0.60		0.794
FeO calc	3.72	0.16	0.618	3.55	0.020	0.596
Fe <sub>2</sub> O <sub>3</sub> calc	9.11	0.28	1.364	9.04	0.078	1.364
Total FeCalc	100.36	0.32		99.78	0.088	

See text for explanation of calculated (calc) quantities. The "type grain" is the grain of greenwoodite that single crystal XRD data was collected from.

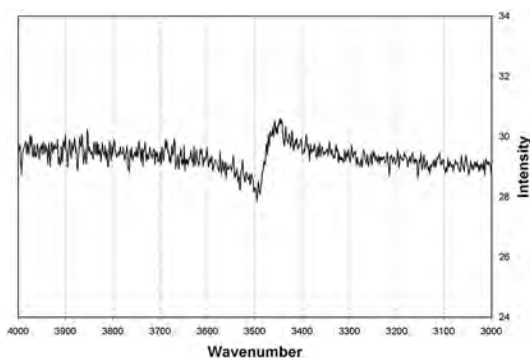


FIG. 2. FTIR spectrum from a greenwoodite grain showing an O-H stretching vibration absorption peak at about 3495 cm<sup>-1</sup>.

APEX II CCD detector and a  $K\alpha$ Mo radiation source. A hemisphere of data was collected for  $2.8^\circ \leq 2\theta \leq 60.20^\circ$  using frame widths of  $0.3^\circ$  in  $\omega$ , with 10 seconds/frame yielding a total of 7901 reflections in the triclinic Laue symmetry class  $\bar{1}$ . Initial data processing was performed using Bruker software including absorption corrections using SORTAV (Blessing, 1987) and adopting the spherical approximation:  $\mu = 9.122 \text{ mm}^{-1}$  and  $T_{\text{min}} - T_{\text{max}} = 0.4819 - 0.4917$  (see also Table 3). The complete reflection statistics ( $R_{\text{int}} = 3.3\%$ ) supported the trigonal space group  $P\bar{3}m1$  (Laue class  $\bar{3}m$ ). The  $|E^2 - 1|$  for all data, 0.957, fits the theoretical value for a centrosymmetric space group. Merging of the equivalents resulted in 515 unique reflections, of which 475 are considered

observed ( $|F_o| \geq 4\sigma_F$ ). A single orientation matrix was identified that gave a hexagonal unit cell with  $a = 5.750(1)$  and  $c = 14.459(1)$  Å. Following single-crystal data collection, the greenwoodite grain this data was collected from was re-mounted and polished for microprobe analysis; the results are tabulated separately in Table 2, identified as "Type grain".

The initial structure solution was performed using direct methods (SHELXL-97; Sheldrick 1997, 2008) for the location of heavy atoms Ba, V, and Fe and using Patterson synthesis and Fourier maps for the positions of the Si and O atoms. Refinement of the full anisotropic model for all atoms yielded agreement factors  $R1$  of 2.3% and 1.9%, respectively, for all 515 unique reflections and for the 475 reflections considered observed. The goodness of fit ( $S$ ) was 1.015. A summary of the structure solution parameters is presented in Table 3. The final atom coordinates and the  $U_{\text{eq}}$  displacement parameters are presented in Table 4; bond lengths, polyhedral volumes, and distortion parameters are in Table 5; bond-valence sums are in Table 6; and the anisotropic displacement parameters are in Table 8 (deposited).

#### Structure Description

Greenwoodite has a structure based on a hexagonal closest packing (hcp) of anions (oxygen) with a stacking sequence ...ababab.... Variations in the type and coordination of cations occupying interstices between pairs of h-stacked anion layers result in 4 distinct cation layers, which are designated here as BV, V1, V2, and V3. The stacking sequence of these layers is BV-V1-V2-V3-V2-V1-BV-V1-.... The structure contains 6 distinct oxygen sites (O1 through O6), one tetrahedral Si site

(SiT), one Fe-dominated tetrahedral site (FeT), one cubo-octahedral Ba site (Ba), and 4 distinct vanadium-dominated octahedral sites (V1, V2, V3, and V4). The V1, V2, and V3 layers contain only V1, V2, and V3 octahedral sites, respectively.

The V1 layer (V1 cation on the three-fold axis) is a mixed layer built up from corner sharing octahedra and SiO<sub>4</sub> tetrahedra (Si on the three-fold axis) in which each octahedron is connected to three surrounding tetrahedra and only half of the tetrahedral positions are occupied (pointing in the same direction).

The V3 layer (V3 at the inversion center) is a mixed layer built up from corner-sharing octahedra and FeO<sub>4</sub> tetrahedra (Fe on the three-fold axis). The arrangement

of octahedra is equivalent to the V1 layer but all the interstitial tetrahedral position are occupied and the tetrahedra point alternatively up and down

Sandwiched between V1 and V3 layers is the V2 octahedral layer (V2 in general position); it is a derivative CdI<sub>2</sub>-type oxide/spinel octahedral layer in which every third octahedral cavity is empty and each V2 octahedra shares edges with the other four surrounding octahedra. Three adjacent V2 octahedra share common corners at O1 and at O2 which are, respectively, the apical corner of the "pointing-up" FeO<sub>4</sub> tetrahedra in the adjacent V3 layer and the apical corner of the SiO<sub>4</sub> tetrahedra in the adjacent V1 layer. The basal face of the "pointing-down" FeO<sub>4</sub> tetrahedra is positioned adjacent to the empty octahedra.

The average greenwoodite structure displays disorder in the BV layer, which can be described as a disordered mixture of two versions of this cation layer, which are referred to as the Ba phase and the VOH phase. In the Ba phase both bounding hcp anion planes of the BV layer (basal to the adjacent V1 layers) are missing one in every four anions per unit cell, forming cubo-octahedral cavities between adjacent mirror-related anion layers that are occupied by twelve coordinate Ba (Ba at the missing anion position; see Fig. 3). In the VOH phase the same anion position (occupied by Ba in the Ba phase) is occupied by oxygen (O6), which forms the central shared-corner of a triplet of edge-sharing V4 octahedra (Fig. 4). Topologically there is one of these octahedral triplets for every Ba position in the Ba phase, but, since every V4 octahedron is shared between two triplets, the VOH phase has three V4 octahedra per unit cell in place of the two Ba per unit cell in the Ba phase. Both site occupancy results and compositional data indicate that only two of every three V4 octahedra is occupied. Although the structure refinement did not identify the location of H, charge

TABLE 3. STRUCTURE SOLUTION DATA FOR GREENWOODITE

Crystal size (μm)	100 × 70 × 50
Space Group	<i>P</i> $\bar{3}$ <i>m</i> 1
<i>a</i> (Å)	5.7500(6)
<i>c</i> (Å)	14.4590(9)
<i>V</i> (Å <sup>3</sup> )	414.00(8)
<i>Z</i>	1
Calculated density (g/cm <sup>3</sup> )	4.81
Wavelength (Å)	0.71070
μ (mm <sup>-1</sup> )	9.122
<i>T</i> <sub>min</sub>	0.4819
<i>T</i> <sub>max</sub>	0.4917
Scan mode Δω=Δφ(°)	0.3
<i>T</i> (K)	293
2θ <sub>max</sub> (°)	60.2
<i>hkl</i> <sub>(total)</sub>	7901
<i>hkl</i> <sub>(unique)</sub>	515
<i>hkl</i> <sub>(unique)</sub> (  <i>F</i> <sub>0</sub>   > 4σ <i>F</i> <sub>0</sub> )	475
<i>R</i>	0.020
Variable parameters	55

TABLE 4. ATOMIC COORDINATES AND OCCUPANCY FACTORS FOR THE GREENWOODITE STRUCTURE

Site	Multiplicity	<i>x</i>	<i>y</i>	<i>z</i>	<i>U</i> <sub>eq</sub> *	Occupancy
Ba	2	1/3	2/3	0.06805(4)	0.0148(2)	0.618(3)
O6	2	1/3	2/3	0.06805(4)	0.0148(2)	0.382(3)
V1	2	2/3	1/3	0.17733(6)	0.0051(2)	1
V2	6	0.18382(6)	0.36765(11)	0.32518(3)	0.0055(1)	1
V3	1	0	0	1/2	0.0054(2)	1
V4	3	1/2	0	0	0.0289(13)	0.270(4)
FeT	2	1/3	2/3	0.55041(6)	0.0065(2)	1
SiT	2	0	0	0.13003(10)	0.0088(4)	1.133(9)
O1	2	1/3	2/3	0.4172(3)	0.0074(7)	1
O2	2	0	0	0.2499(2)	0.0064(7)	1
O3	6	0.3031(5)	0.1515(2)	0.40902(15)	0.0073(4)	1
O4	6	0	1/2	0.25157(15)	0.0078(4)	1
O5	6	0.3202(6)	0.1601(3)	0.09610(18)	0.0172(5)	1

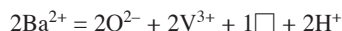
\* *U*<sub>eq</sub> = B/8π<sup>2</sup>

balance requirements of the VOH phase imply that there is one H for each O6 and bond-valence sums (Table 6) imply that each H is bonded to each O6 as OH<sup>-</sup>. The VOH layer is another CdI<sub>2</sub>-type oxide layer (or Kagomé OC<sub>3</sub>-type layer), topologically identical to the V2-layer.

### Structural Formula and Site Occupancies

Although the microprobe analyses report minor amounts of Cr, Ti, Zn, Al, Mn, and Mg, greenwoodite is primarily a compound of Ba, V, Fe, Si, O, and H. As indicated by the structure description above, the "ideal" formula for greenwoodite must be expressed in terms of two endmembers that have identical core structures (layers V1, V2, and V3) and 100% of each of the Ba and VOH versions of the BV layer. Bond-valence sums (Table 6) and comparison of octahedral ionic radii of V ions (Shannon 1976) with average bond lengths for the V1, V2, V3, and V4 sites (Table 5, minus 1.40 for O<sup>2-</sup>) both imply that V is present primarily as V<sup>3+</sup>. Charge balance in the core layers can only be achieved if half of the Fe at the FeT site is Fe<sup>3+</sup> and half is Fe<sup>2+</sup>. While

this is unusual, it is not unlike the disordered sharing of the same site by equal amounts of Si and Al in gehlenite (*e.g.*, Louisnathan 1971). Average bond length data (Table 5) and the bond-valence sum data (Table 6) both support this division of Fe valence states. As mentioned above, the coupled-substitution reaction that would allow the Ba phase to mix with the VOH phase will only be charge-balanced if there exists one H for each O6 oxygen as follows:



where  $\Box$  symbolizes the vacancy of one V4 site out of every triplet of V4 sites. Given the unit-cell multiplicity factors for each cation and oxygen site, the formula of the Ba phase is then: Ba<sub>2</sub>V<sub>9</sub>(Fe<sup>3+</sup>,Fe<sup>2+</sup>)<sub>2</sub>Si<sub>2</sub>O<sub>22</sub> and the formula of the VOH phase is (VOH)<sub>2</sub>V<sub>9</sub>(Fe<sup>3+</sup>,Fe<sup>2+</sup>)<sub>2</sub>Si<sub>2</sub>O<sub>22</sub>. The ideal formula for the observed disordered mixture of these two phases is therefore Ba<sub>2-x</sub>(VOH)<sub>x</sub>V<sub>9</sub>(Fe<sup>3+</sup>,Fe<sup>2+</sup>)<sub>2</sub>Si<sub>2</sub>O<sub>22</sub>. Although there is utility in the structure description above to talk about the Ba

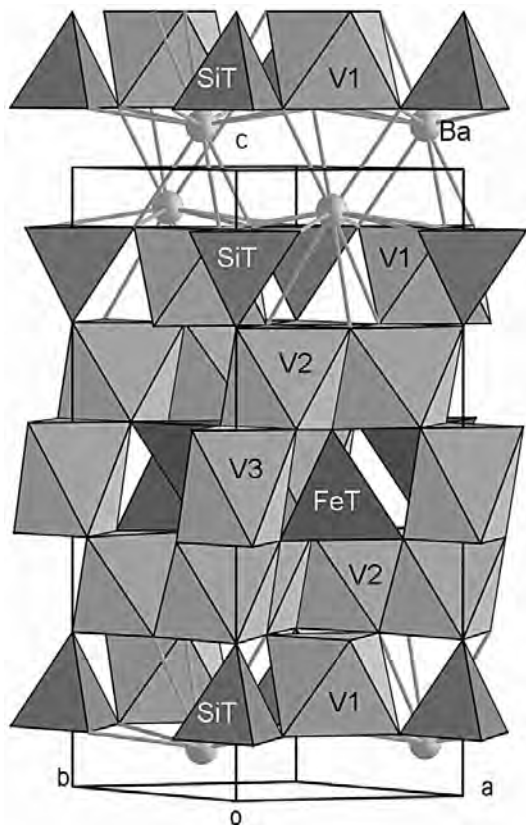


FIG. 3. Polyhedral representation of the Ba-phase structure of greenwoodite. See text for explanations.

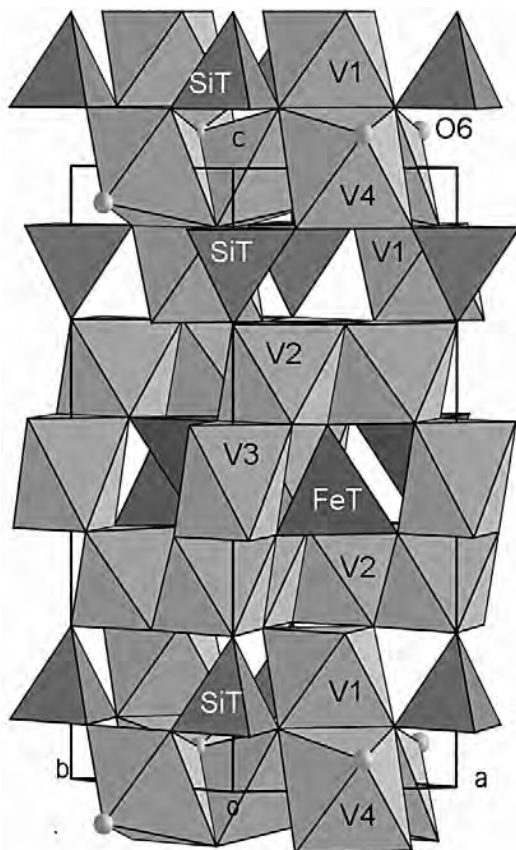


FIG. 4. Polyhedral representation of the VOH-phase structure of greenwoodite. See text for explanations.

TABLE 5. BOND LENGTHS, POLYHEDRAL VOLUMES AND DISTORTION PARAMETERS

Ba	O5	2.904(1)	V1	O4	1.977(2)	V3	O3	2.003(2)	
	O5	2.904(1)		O4	1.977(2)		O3	2.003(2)	
	O5	2.904(1)		O4	1.977(2)		O3	2.003(2)	
	O5	2.904(1)		O5	2.087(3)		O3	2.003(2)	
	O5	2.904(1)		O5	2.087(3)		O3	2.003(2)	
	O5	2.904(1)		O5	2.087(3)		O3	2.003(2)	
	O5	2.934(3)	mean		<b>2.032(2)</b>	mean		<b>2.003(2)</b>	
	O5	2.934(3)	Vol		11.1564	Vol		10.3985	
	O5	2.934(3)	quad. elong		1.0026	quad. elong		1.0205	
	O4	3.130(2)	angle var.		6.5472	angle var.		78.7836	
	O4	3.130(2)	$\Delta$		0.0007	$\Delta$		0.0000	
	O4	3.130(2)							
	mean		<b>2.968(2)</b>	V2	O4	1.906(1)	FeT	O3	1.903(2)
					O4	1.906(1)		O3	1.903(2)
				O1	1.997(1)		O3	1.903(2)	
V4	O6	1.929(1)		O3	2.082(1)		O1	1.926(4)	
	O6	1.929(1)		O3	2.082(1)	mean		<b>1.908(2)</b>	
	O5	2.190(2)		O2	2.129(2)	Vol		3.5639	
	O5	2.190(2)	mean		<b>2.062(2)</b>	quad.elong		1.0006	
	O5	2.190(2)	Vol		10.7500	angle var.		2.7406	
	O5	2.190(2)	quad.elong		1.0137	$\Delta$		0.0000	
	mean		<b>2.103(1)</b>	angle var.	40.6003				
	Vol		12.3148	$\Delta$	0.0023	SiT	O5	1.668(3)	
	quad.elong		1.0086				O5	1.668(3)	
	angle var.		6.0181				O5	1.668(3)	
$\Delta$		0.0034				O2	1.734(4)		
						mean	<b>1.685(3)</b>		
						Vol	2.4485		
						quad.elong	1.0016		
						angle var.	6.613		
						$\Delta$	0.0003		

TABLE 6. BOND VALENCE TABLE ( $\nu u$ ) FOR GREENWOODITE

	Ba	V1	V2	V3	V4	SiT	FeT	$\Sigma$
O1			0.504				0.636	2.148
O2			0.352			0.743		1.798
O3			0.400	0.495			0.678	1.973
O4	0.102	0.531	0.644					1.921
O5	0.183	0.395			0.298	0.887		1.830
O6					0.604			1.208
$\Sigma$	1.949	2.778	2.944	2.967	2.401	3.403	2.671	

phase and the VOH phase, these correspond to the Ba-endmember and VOH-endmember of the mixed (solid solution) phase.

Given the structural formula and the implied direct relationship between the number of Ba atoms (per formula unit) and the proportion of the Ba-endmember, the microprobe analyses of the type grain of greenwoodite put its position in the solid solution at 60% of the Ba-endmember. Site occupancy factors from the

structure refinement (Table 4) for the Ba and O6 sites (restricting their sum to be 1.0) are consistent with this figure. Microprobe analyses from additional grains of greenwoodite span the range from 54% to 64% of the Ba phase. Within the context that each half of the full range of a binary solid solution is recognized as a distinct mineral species, greenwoodite corresponds to the Ba-rich half of the Ba-VOH solid solution.

Occupancy of the cation sites in greenwoodite by the minor elements in the microprobe analyses (Cr, Ti, Zn, Al, Mn, and Mg) was modeled as follows:

**SiT Site:** The microprobe analyses consistently contain an amount of Si that is 12–14% less than that required to fill the SiT site and an amount of Al that is close to the amount required to fill this site. While it is common in silicates for a minor amount of Al to replace Si, there are two lines of evidence that indicate that another element other than Al must be occupying the SiT site: (1) A plot of Al against Si (APF) for all of the microprobe analyses does not show the anti-correlation expected if Al was the primary filler of the Si site, and (2) the site occupancy factor for the Si site from the structure refinement (Table 4) is 13% greater than 1.0, indicating the minor presence of a cation with a scattering power significantly greater than that of Si. Of all of the candidates (other than Al) in the microprobe analysis that are known to occur in tetrahedral coordination, the two that are closest to Si in (tetrahedral) ionic radii are  $Ti^{4+}$  and  $Fe^{3+}$ . As seen in minerals like schorlomite (*e.g.*, Peterson *et al.* 1995), the preference of  $Ti^{4+}$  for octahedral sites makes it more likely that  $Fe^{3+}$  is partially occupying the Si site. Presuming the Si site to be fully occupied in general, the model for this site in natural greenwoodite is: all Si +  $Fe^{3+}$  to fill the site. Table 7 shows both observed average cation radii and the refined number of electrons per site compared with calculated quantities based upon the occupancy assignments. The level of agreement for the SiT site lends support to the site occupancy model described above.

**FeT Site:** The site occupancy model for the FeT site seeks to both assign minor elements to the site and assign proportions of  $Fe^{3+}$  and  $Fe^{2+}$ .

With  $Fe^{3+}$  in the SiT site ( $Fe_{SiT}$ ) reducing the total cation charge at the SiT site and  $Ti^{4+}$  creating an excess cationic charge at the octahedral sites (dominated by +3 cations; see below) the excess cationic charge external to the FeT site (EC) is equal to  $Ti^{4+} - Fe_{SiT}$ . To maintain overall charge balance the proportions of divalent cations at the FeT site ( $C_{2FeT}$ ) and trivalent cations ( $C_{3FeT}$ ) must shift an amount equal to EC where (in

atoms per formula):  $C_{2FeT} = 1 + EC$  and  $C_{3FeT} = 1 - EC$ . For all the microprobe compositions EC is between  $-0.10$  and  $-0.16$ .

The Zn in greenwoodite is likely to prefer the FeT site, since the octahedral ionic radius of Zn is larger than any of the octahedral sites in greenwoodite and experience with another structure with tetrahedral Fe (staurolite) also shows a preference of minor Zn for the tetrahedral Fe site (*e.g.*, Hawthorne *et al.* 1993, Griffen *et al.* 1982). The small amount of Mg in greenwoodite is also being modeled as occupying the FeT site. Since these are both divalent cations the total amount of  $Fe^{2+}$  (at the FeT site) is  $C_{2FeT} - Zn - Mg$ .

The remaining Fe in the microprobe analyses was assigned to the FeT site as  $Fe^{3+}$ , *i.e.*,  $Fe_{3FeT} = Fe_{total} - Fe_{SiT} - Fe^{2+}$ . For all but one of the analyses  $Fe_{3FeT}$  is slightly less than  $C_{3FeT}$ . As the only minor element with some likelihood of occurring at a tetrahedral site, the remainder of the FeT site was filled with Al. In Table 7 both observed average cation radius and the refined number of electrons show good agreement with calculated quantities based upon this site occupancy model for FeT.

**Octahedral Sites:** The octahedral sites in greenwoodite, while dominated by  $V^{3+}$ , are being modeled as also containing all  $Ti^{4+}$  (see above), all Cr as  $Cr^{3+}$ , all Mn as  $Mn^{3+}$ , and the Al that is not required to fill the FeT site (see above), with the exception of V4. A plot of V against Cr from the microprobe analyses shows a strong anti-correlation that supports the conclusion that these two elements are exchanging with each other at a common site or sites. However, a plot of Cr against the amount of V4 sites available (as percent of the VOH-endmember) does not show any correlation, implying that Cr may not have a significant presence at the V4 site. As a result, the V4 site is being modeled here as containing only  $V^{3+}$ . The Cr, Mn, Ti, and non-tetrahedral Al are being modeled as equally distributed among V1, V2, and V3, since there is insufficient data to develop a rational model for placement of these minor elements in each of these sites individually. However, since these minor (octahedral) elements all have ionic radii smaller than that of  $V^{3+}$ , they are likely to be concentrated to some degree at V3, the smallest octahedral site.

The comparison of observed and calculated cation radii and cation electrons in Table 7 shows variable agreement for V1, V2, and V3 individually, but good agreement with these sites averaged as a group. The agreement for the V4 site is not as good, especially for the observed and calculated ionic radii. Note, however, that not only is the observed V4 site slightly larger than a  $V^{3+}$  ion, but the observed Ba site is slightly smaller than a 12-coordinated  $Ba^{2+}$  ion. Both of these misfits may result from the fact that the refined atomic positions in the BV layer of the structure are an average of the Ba version of this layer and the VOH version of this layer.

TABLE 7. OBSERVED AND CALCULATED MEAN IONIC RADII AND NUMBER OF ELECTRONS FOR THE CATION SITES OF THE GREENWOODITE STRUCTURE

Site	Radius (Å) (obs.)	Radius (Å) (calc.)	e- (obs.)	e- (calc.)
Ba	1.568	1.61	33.4	32.4
V1	0.632	0.632	20.0	19.7
V2	0.662	0.632	20.0	19.7
V3	0.603	0.632	20.0	19.7
V4	0.703	0.640	5.4	5.3
FeT	0.508	0.543	23.5	23.2
SiT	0.285	0.292	11.3	11.8



Given all of the above considerations, the empirical formula of the type grain of greenwoodite is:  $\text{Ba}_{1.20}(\text{VOH})_{0.80}(\text{V}_{8.33}, \text{Cr}_{0.33}, \text{Ti}_{0.13}, \text{Al}_{0.13}, \text{Mn}_{0.02})_{\Sigma 9}(\text{Fe}^{3+})_{1.08}, \text{Fe}^{2+}_{0.60}, \text{Zn}_{0.22}, \text{Al}_{0.06}, \text{Mg}_{0.04})_{\Sigma 2}(\text{Si}_{1.72}, \text{Fe}^{3+}_{0.28})_{\Sigma 2}\text{O}_{22}$

#### Powder X-ray Data

Because of the small amount of material available, X-ray powder diffraction data were not collected independently. The powder pattern was calculated using the program XPOW (Downs *et al.* 1993), based on the structure analysis. X-ray powder diffraction data (in Å for  $\text{CuK}\alpha$ ) are given in Table 9.

#### DISCUSSION

According to the new Dana classification (Hurlbut and Edwin Sharp 1998) greenwoodite belongs to the 53.02 class, nesosilicates - insular  $\text{SiO}_4$  groups and other anions of complex cations with  $(\text{SO}_4)$ ,  $(\text{CrO}_4)$ ,  $(\text{PO}_4)$  etc., because it contains  $\text{FeO}_4$  as a complex cation. According to the Strunz classification (Strunz 1996) greenwoodite belongs to the 09.AH class, nesosilicates with  $\text{CO}_3$ ,  $\text{SO}_4$ ,  $\text{PO}_4$ .

The greenwoodite structure can be characterized as a stacking of  $\text{CdI}_2$ -type oxide layers (V2 and V4 layers), interleaved by  $\text{TeOC}$  layers (V1) with half of the tetrahedra empty and  $\text{Te}_2\text{OC}$  layers (V3) with all tetrahedral positions occupied. There are several compounds whose structures are formed by stacking of the same building blocks. For instance, some barium cobaltite compounds,

*i.e.*,  $\text{Ba}_2\text{Co}_4\text{ClO}_7$  and  $\text{Ba}_2\text{Co}_4\text{BrO}_7$ , have structures that can be described as intergrowths of  $\text{CdI}_2$ -type and perovskite layers connected through "interface" mixed layers  $\text{TeOC}$  and  $\text{Te}_2\text{OC}$ . It is particularly interesting to note that a group of Ba-Sn ferrite compounds with the formula  $\text{Ba}_2\text{Sn}_2\text{MeFe}_{10-x}\text{Ga}_x\text{O}_{22}$  (where Me is a divalent transition metal) are isostructural with the Ba-endmember of the greenwoodite structure. The description of the structure of these compounds (Cadée *et al.* 1986) even shows that, in some cases such as  $\text{Ba}_2\text{Sn}_2\text{MnFe}_{10}\text{O}_{22}$ , the site equivalent to FeT in greenwoodite contains approximately 50%  $\text{Fe}^{3+}$  and 50% of divalent metal ( $\text{Mn}^{2+}$ ) very similar to the occupancy of FeT in greenwoodite.

Greenwoodite displays an unusual form of solid solution in that a cation (Ba) is replaced by an anion (O) and one endmember has cation sites that the other endmember does not. Some similarities can be seen in other hcp oxide structures having a large Ba site formed by a hole in one of the oxygen layers. Barian tomichite [ideal formula  $\text{Ba}_{0.5}(\text{As}_2)_{0.5}\text{Ti}_2\text{V}_5\text{O}_{13}(\text{OH})$ ] can be modeled as a mixture of a Ba-structure where Ba occupies the large site and an  $\text{As}_2$ -structure where a bonded pair of As occupies the Ba site and no atom is centered at the same position as Ba in the Ba-structure (Grey *et al.* 1987). In batisvite (ideal formula  $\text{V}_8\text{Ti}_6[\text{Ba}(\text{Si}_2\text{O}_7)]\text{O}_{22}$ ), an example of which occurs with greenwoodite, Ba at the large site is also replaced by an O anion, however, in this case, this O anion forms the shared corner of a  $\text{Si}_2\text{O}_7$  pair of Si tetrahedra that occupy the space formerly occupied by one Ba (Armbruster *et al.*

TABLE 9. CALCULATED POWDER XRD DATA FOR GREENWOODITE

$d_{calc}$	$l_{calc}$	$hkl$	$d_{calc}$	$l_{calc}$	$hkl$
14.459	12	0 0 1	1.847	2	1 1 6
4.980	3	1 0 0	1.821	5	1 2 2, 2 1 2
4.820	5	0 0 3	1.807	3	0 0 8
4.708	11	0 1 1, 1 0 1	1.753	1	1 2 3, 2 1 3
4.101	2	0 1 2, 1 0 2	1.732	5	0 2 6, 2 0 6
3.615	2	0 0 4	1.699	8	0 1 8, 1 0 8
3.463	3	0 1 3, 1 0 3	<b>1.669</b>	<b>26</b>	<b>1 2 4, 2 1 4</b>
<b>2.925</b>	<b>100</b>	0 1 4, 1 0 4	1.660	6	3 0 0
2.892	6	0 0 5	1.649	3	0 3 1, 3 0 1
<b>2.875</b>	<b>38</b>	1 1 0	1.618	6	0 3 2, 3 0 2
2.820	3	1 1 1	1.590	23	0 2 7, 2 0 7
<b>2.672</b>	<b>23</b>	1 1 2	1.577	6	1 2 5, 2 1 5
2.501	4	0 1 5, 1 0 5	1.569	9	0 3 3, 3 0 3
2.490	6	2 0 0	1.530	3	1 1 8
<b>2.469</b>	<b>35</b>	1 1 3	1.529	1	0 1 9, 1 0 9
2.454	10	0 2 1, 2 0 1	1.483	9	2 1 6, 1 2 6
<b>2.354</b>	<b>28</b>	2 0 2, 0 2 2	1.463	20	0 2 8, 2 0 8
<b>2.212</b>	<b>28</b>	2 0 3, 0 2 3	<b>1.438</b>	<b>35</b>	2 2 0
2.169	5	0 1 6, 1 0 6	1.402	3	1 1 9
2.051	17	2 0 4, 0 2 4	1.389	1	1 0 10, 0 1 10
1.887	15	0 2 5, 2 0 5	1.304	3	1 2 8, 2 1 8
1.866	3	1 2 1, 2 1 1			

2008). In both of these cases, however, the extent of the mixture at the Ba site is very close to 50-50 and supercell reflections indicate that the mixture is extensively ordered in an approximately every-other-site arrangement. This ordering may be what stabilizes barian tomichite and batisivite in nature, where neither appears to operate as a solid-solution.

#### ACKNOWLEDGMENTS

Acknowledgement and appreciation are extended to the following individuals for their contribution to this paper: Trygve Høy and the B.C. Geological Survey for contributing the type rock sample; Patricia Metcalf of the Materials Engineering department at Purdue University for contributing pure synthetic  $V_2O_3$  that was used as a microprobe standard; George Rossman for assistance in the interpretation of FTIR spectra; Hugh Greenwood for providing training and mentoring to the first author; Heikki Papunen for guidance and advice to FM; and two anonymous reviewers for their helpful suggestions.

#### REFERENCES

- ARMBRUSTER, T., KADIYSKI, M., REZNITSKY, L.Z., SKLYAROV, E.V., & GALUSKIN, E.V. (2008) Batisivite, the first silicate related to the derbylite-hemloite group. *European Journal of Mineralogy* **20**, 975-981.
- BARTHOLOMEW, P.R., MANCINI, F., CAHILL, C., HARLOW, G., & BERNHARDT, H. (2005) Zoltaiite, a new barium-vanadium nesosubsilicate mineral from British Columbia: description and crystal structure. *American Mineralogist* **90**, 1655-1660.
- BARTHOLOMEW, P.R., MANCINI, F., HARLOW, G.E., CAHILL, C., DEIFEL, N., & BERNHARDT, H. (2010) Greenwoodite, IMA 2010-007. CNMNC Newsletter, June 2010, page 578. *Mineralogical Magazine* **74**, 577-579.
- BLESSING, R.H. (1987) Data reduction and error analysis for accurate single crystal diffraction intensities. *Crystallography Reviews* **1**, 3-58.
- CADÉE, M.C., DE GROOT, H.J.M., DE JONGH, L.J., & IJDO, D.J.W. (1986) Crystal structure and magnetic properties of some new hexagonal ferrites ( $Ba_2Sn_2MeFe_{10-x}Ga_xO_{22}$ ) with the QS-structure. *Journal of Magnetism and Magnetic Materials* **62**, 367-380.
- DOWNES, R.T., BARTELMERHS, K.L., GIBBS, G.V., & BOISEN, M.B., JR. (1993) Interactive software for calculating and displaying X-ray or neutron powder diffractometer patterns of crystalline materials. *American Mineralogist* **78**, 1104-1107.
- GORDON, T.M. (1991) Quantitative methods in petrology – an issue in honor of Hugh J. Greenwood: Preface. *Canadian Mineralogist* **29**, 611-613.
- GREY, I.E., MADSEN, I.C., & HARRIS, D.C. (1987) Barian tomichite,  $Ba_{0.5}(As_2)_{0.5}Ti_2(V,Fe)_5O_{13}(OH)$ , its crystal structure and relationship to derbylite and tomichite. *American Mineralogist* **72**, 201-208.
- GRIFFEN, D.T., GOSNEY, T.C., & PHILLIPS, W.R. (1982) The chemical formula of natural staurolite. *American Mineralogist* **67**, 292-267.
- HAWTHORNE, F.C., UNGARETTI, L., OBERTI, R., CAUCIA, F., & CALLEGARI, A. (1993) The crystal chemistry of staurolite: I. Crystal structure and site populations. *Canadian Mineralogist* **31**, 551-532.
- HURLBUT, C.S. & SHARP, W.E. (1998). *Dana's Minerals and How to Study Them*, 4th edition. John Wiley & Sons, Inc., New York, 328 p.
- LOUISNATHAN, S.J. (1971) Refinement of the crystal structure of a natural gehlenite,  $Ca_2Al(Al,Si)_2O_7$ . *Canadian Mineralogist* **10**, 822-837.
- PETERSON R.C., LOCOCK A.J., & LUTH R.W. (1995) Positional disorder of oxygen in garnet: the crystal-structure, refinement of schorlomite. *Canadian Mineralogist* **33**, 627-631.
- ROSSMAN, G.R. (1988) Vibrational spectroscopy of hydrous components. *Reviews in Mineralogy* **18**, 193-206.
- SHANNON, R.D. (1976) Revised ionic radii and systematic studies of interatomic distances in chalcogenides. *Acta Crystallographica* **A32**, 751-767.
- SHELDRIK, G.M. (1997) *SHELXL-97: A Computer Program for Structure Refinement*. University of Göttingen, Germany.
- SHELDRIK, G.M. (2008) A short history of SHELX. *Acta Crystallographica* **A64**, 112-122.
- STRUNZ, H. (1996) Chemical-structural mineral classification. Principles and summary of system. *Neues Jahrbuch für Mineralogie, Monatshefte* **10**, 435-445.
- THOMPSON, R.I. (1972) *Geology of the Akolkolex River area near Revelstoke, British Columbia*. Ph.D. thesis, Queen's University, Kingston, Ontario, 125 p.
- THOMPSON, R.I. (1978) Geology of the Akolkolex River Area. *British Columbia Ministry of Energy, Mines and Petroleum Resources Bulletin*, 60, 84 p.

Received February 8, 2012, revised manuscript accepted September 24, 2012.